EurJOC
European Journal of Organic Chemistry

Research Article
doi.org/10.1002/ejoc.202101273

Chemistry Europe
European Chemical Societies Publishing

www.eurjoc.org

Special Collection

PAHs Containing both Heptagon and Pentagon: Corannulene Extension by [5+2] Annulation

Matthias Schnitzlein,[a] Carina Mützel,[a] Kazutaka Shoyama,[a] Jeffrey M. Farrell,[a] and Frank Würthner*[a]

In memory of Professor Klaus Hafner

Utilizing Pd-catalyzed [5+2] annulation a series of heptagon-extended corannulenes could be synthesized from a borinic acid precursor furnished by C–H borylation strategy. Single-crystal X-ray analysis revealed the presence of two conformational enantiomers crystallizing in a racemic mixture. Through their embedded five- and seven-membered rings these polycyclic aromatic hydrocarbons (PAHs) exhibit both negative and positive curvature and UV/Vis/NIR absorption spectroscopy as well as cyclic voltammetry experiments provided insights into the influence of larger flanking aromatic systems and electron-donating substituents encompassing the heptagonal ring. Through [5+2] annulation of acenaphthylene an azulene-containing PAH with intriguing optoelectronical properties including a very small bandgap and absorption over the whole visible spectrum could be obtained. Theoretical calculations were employed to elucidate the long-wavelength absorption and aromaticity.

Introduction

Polycyclic aromatic hydrocarbons (PAHs) are unsaturated two-dimensional carbon frameworks that resemble substructures of graphene.[1] Through inclusion of non-hexagonal rings PAHs exhibit distinctive optoelectronic properties. Fusing seven-membered rings onto five-membered rings leads to azulene moieties as described by Klaus Hafner in his "rational synthesis of azulene" in the 1950s.[2] More recently, a plethora of azulene-containing PAHs have been synthesized.[3] On the other hand, incorporation of isolated non-hexagonal rings can lead to a warped, three-dimensional structure resulting in higher solubility. Whereas inclusion of five-membered rings into PAHs generally leads to positive curvature and a bowl shape, embedded seven-membered rings mostly result in negative curvature and a saddle-shape.[4] Surprisingly, to date only few PAHs containing both types of curvature are known.[5] Often problematic is the synthesis of seven-membered rings, which suffer a lack of general synthetic methods. For such operations, mostly oxidative coupling is used and thus the reaction scope is narrow.[6] The hitherto employed approaches involve functionalization of positively curved corannulene[7] with subsequent cross-coupling of suitable precursors to provide the prearranged scaffold for oxidative seven-membered ring formation.[5] In order to develop a more general synthetic method for both positively and negatively curved PAHs, we have conjected that [5+2] annulation of styrene-substituted corannulene **3** and suitable PAH could produce a series of such curved π-conjugated carbon materials.

Herein, we report the synthesis and characterization of heptagon-extended corannulenes **1a–d** bearing both negative and positive curvature. Our synthetic procedure consists of one-pot hydroboration electrophilic borylation cascade and follow-up dehydrogenation of simple alkenes to borinic acids[8] and subsequent palladium-catalyzed [5+2] annulation with suitable aryl dihalides.[9] Furthermore, this methodology could also be used for the synthesis of an azulene-containing PAH by fusing acenaphthylene,[3h] which exhibited long-wavelength absorption that is unusually red-shifted for pure hydrocarbons with similar size.

Results and Discussion

We first synthesized styrylcorannulene **3** following the route developed by Stuparu and coworkers.[10,11] Corannulene aldehyde **2** could be efficiently generated in multi-gram scale by Rieche formylation.[10] Subsequent Horner-Wadsworth–Emmons (HWE) reaction of aldehyde **2** with benzyl diethyl phosphonate and potassium *tert*-butoxide yielded alkene **3**.[11] Borinic acid **5**, which served as precursor in the final [5+2] annulation, was prepared using our previously reported NHC-mediated C-H borylation strategy[8] and was obtained in 21% yield. Under [5+2] coupling conditions with two equivalents of the respective *ortho*- dibromoarene **6a–d**, $[Pd_2(dba)_3]\cdot CHCl_3$ as palladium precatalyst, $P(^tBu)_3\cdot HBF_4$ as ligand, cesium carbonate as base

[a] M. Schnitzlein, C. Mützel, Dr. K. Shoyama, Dr. J. M. Farrell, Prof. Dr. F. Würthner
Institut für Organische Chemie and Center for Nanosystems Chemistry (CNC), Universität Würzburg
Am Hubland, 97074 Würzburg, Germany
E-mail: wuerthner@uni-wuerzburg.de

Supporting information for this article is available on the WWW under https://doi.org/10.1002/ejoc.202101273

Part of the "Carbon Allotropes" Special Collection.

Research Article
doi.org/10.1002/ejoc.202101273

and water as additive in *tert*-amyl alcohol at 100 °C with 42 h reaction time the PAHs **1 a–d** were obtained in 19–33% yield.

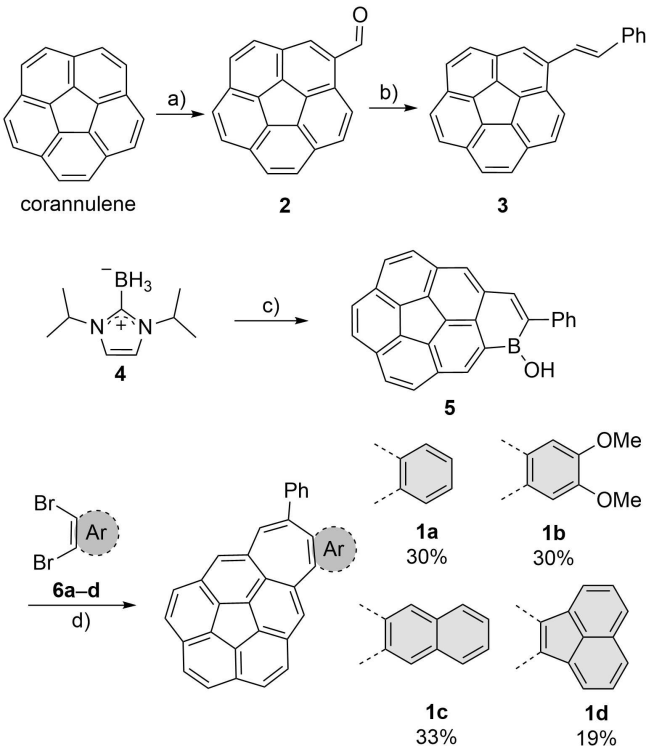

Scheme 1. Synthesis of heptagon-embedded corannulenes **1 a–d**. Conditions: a) Cl_2HCOCH_3, $TiCl_4$, CH_2Cl_2, 16 h, rt, 90%. b) $BnPO(OEt)_2$, KO^{t}Bu, THF, 0 °C to rt, 2.5 h, 89%. c) i) $HNTf_2$, PhCl, rt, 90 min ii) **3**, PhCl, 130 °C, 6.5 h iii) TEMPO, PhCl, 80 °C, 24 h, 21% for three steps d) dibromoarene (2.0 equiv.), $[Pd_2(dba)_3]\cdot CHCl_3$ (5 mol%), $P(^tBu)_3\cdot HBF_4$ (11 mol%), Cs_2CO_3 (3.3 equiv.), H_2O (40 equiv.), ^{t}AmOH, 100 °C, 42 h. Bn: benzyl, TEMPO: 2,2,6,6-tetramethylpiperidinyloxyl, dba: dibenzylideneacetone.

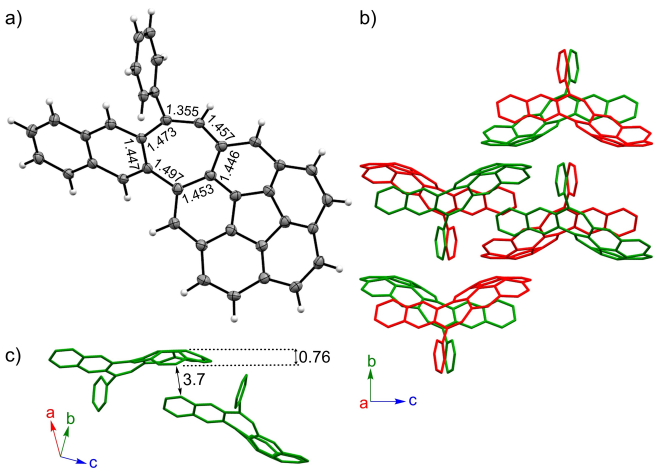

Figure 1. Molecular structure and packing of **1 c** in the crystal. a) Front view with ellipsoids at 50% probability and bond lengths of seven-membered ring. b) Crystal packing along the *a*-axis in a single unit cell. c) C–H-π interaction between two homochiral molecules. Enantiomers are color-coded red and green and hydrogen atoms were omitted for clarity (except in a). All distances and lengths are given in Å.

All compounds are bench-stable for extended time periods and exhibit good solubility in common organic solvents (Scheme 1).

Due to its high thermal stability single crystals of **1 c** could be obtained by sublimation. The crystal structure confirmed the highly warped structure with its positive curvature on the corannulene and the negatively curved seven-membered ring tilting the naphthalene moiety away from the corannulene's bowl (Figure 1).[12] The bowl of **1 c** is only 0.76 Å deep and thus shallower than corannulene which has a bowl depth of 0.87 Å.[13] In the seven-membered ring the length of the shortest bond accounts to 1.355(4) Å (Figure 1a), which corresponds to the length of a conjugated double bond (–C=C–, 1.339 Å).[14] The high double bond character of this bond is also observed in the NMR spectrum, where its proton signal is up-field shifted to 7.09 ppm with regards to its other protons. The further six bonds in the seven-membered ring range between 1.445(4)–1.497(4) Å, which is comparable to single bonds between aromatic systems (–C_{ar}–C_{ar}–, 1.490 Å)[14] and significantly longer than aromatic C–C bonds (–C_{ar}≃C_{ar}–, 1.397 Å).[14] The unit cell of the orthorhombic crystal system within the *Pbca* space group contains eight molecules in four pairs of enantiomers as highlighted in red and green in Figure 1b. Each neighboring homochiral pair has no stacking interaction between them, but C–H-π interactions between the corannulene rim and the outer naphthalene moiety (Figure 1c). With so few attractive interactions between the molecules the good solubility of **1 c** can be rationalized.

In the crystal structure of **1 c**, the annulated naphthalene moiety and the corannulene bowl were located on the same side of the seven-membered ring (here we call it *cisoid* conformation). It is also possible for **1 c** to adopt a *transoid* shape, where the naphthalene and corannulene moieties are opposed to each other in the seven-membered ring. Furthermore, a racemic mixture of *cisoid* enantiomers was present in the crystal. We investigated these phenomena by DFT calculations (Figure 2). Geometry optimized *cisoid* conformation was more stable than the *transoid* one by 21 kJ/mol. A transition state (TS1) featuring a planarized corannulene could be found between the two geometries which was higher in energy by 49 and 28 kJ/mol than the *cisoid* and *transoid* conformations, respectively. Interestingly, we also found a second transition state (TS2) between the *transoid* conformation and the enantiomeric *cisoid* conformation. Both conformations interconvert through ring inversion of the seven-membered ring with a barrier of 19 kJ/mol from the *transoid* and 40 kJ/mol from the *cisoid* geometries. Thus, it is to be expected that a molecule of **1 c** with (*M*)-*cisoid* conformation that converted to the *transoid* conformation through inversion of corannulene rapidly decays to the (*P*)-*cisoid* conformation through TS2 (Figure 2). We therefore assume that in solution at room temperature both conformers are rapidly interconverting in an equilibrium favoring the thermodynamically more stable *cisoid* conformation.Electrochemical studies revealed one oxidation process for **1 a–d** (Table 1). For benzo-fused **1 a** a moderately low oxidation potential of +0.73 V vs. ferrocene/ferrocenium was measured. The same value was obtained for naphthalene-annulated **1 c** indicating that a larger flanking π-system on the seven-

Research Article
doi.org/10.1002/ejoc.202101273

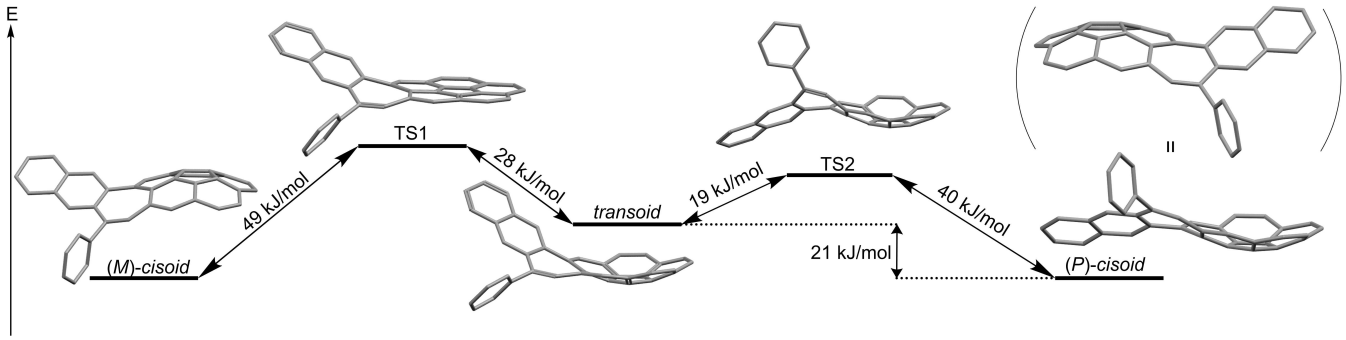

Figure 2. Calculated energy levels of interconversion between the (*M*)-*cisoid* conformation of **1 c**, its *transoid* conformation and its enantiomeric (*P*)-*cisoid* conformation on the B3LYP/6-31 + G(d) level of theory.

Table 1. Optical and redox properties of compounds **1 a**–**d**.

	λ_{abs}[nm] (ε [$M^{-1}cm^{-1}$])[a]	λ_{em} [nm][b] (Φ_{fl})[c]	E_{ox} [V][d]	E_{red} [V][d]
1 a	292 (57300), 403 (10100)	481 (0.21)	+0.73	n.d.
1 b	296 (48300), 422 (9600)	479, 501 (0.24)	+0.53	n.d.
1 c	298 (61500), 406 (13300)	468, 486 (0.30)	+0.73	n.d.
1 d	312 (24800), 371 (26000), 515 (8300), 729 (3200)	n.d.	+0.31	−1.36 −1.92

[a] UV/Vis/NIR spectra were measured in chloroform ($c \approx 1 \times 10^{-5}$ M) at 298 K. [b] Fluorescence spectra were measured in chloroform ($c \approx 1 \times 10^{-7}$ M) at 298 K with the highest wavelength absorption maxima as excitation wavelength. [c] Absolute fluorescence quantum yields were measured in chloroform ($c \approx 1 \times 10^{-5}$ M) at 298 K. [d] CV and DPV spectra were measured at room temperature in dry, degassed dichloromethane ($c \approx 2.5 \times 10^{-4}$ M) with 0.1 M $(n\text{-Bu})_4NPF_6$ under an argon atmosphere and are calibrated to the ferrocene/ferrocenium redox couple. n.d. = not detected.

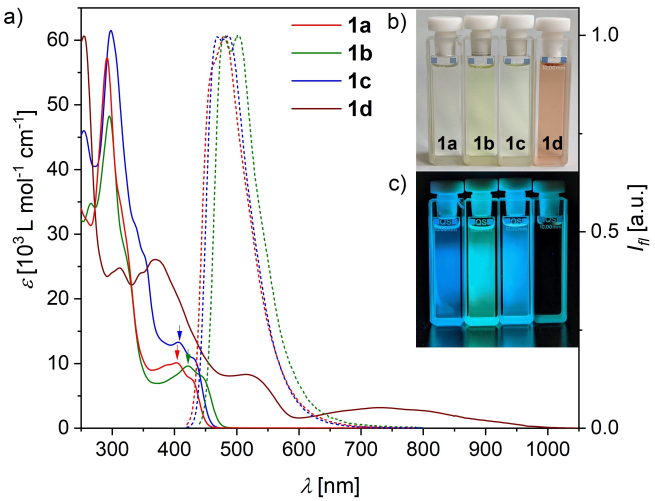

Figure 3. a) UV/Vis spectra (solid lines) and normalized fluorescence emission (dashed lines) of compounds **1 a**–**d**. UV/Vis and fluorescence spectra were measured at 298 K in chloroform ($c \approx 1 \times 10^{-5}$ M for UV/Vis, $c \approx 1 \times 10^{-7}$ M for fluorescence) with the highest wavelength absorption maxima used as excitation wavelength (indicated by the colored arrows). For **1 d** no fluorescence was detected. b, c) **1 a**–**d** (left to right) as $CHCl_3$ solutions under ambient conditions (b) and under UV irradiation (365 nm) (c).

membered ring has a minuscule influence on the electronic properties. Substitution of the heptagon's annulated benzene ring with two electron-donating methoxy groups as in the case of **1 b** significantly decreases the potential to +0.53 V. These potentials are similar to those reported by Miao and coworkers for a saddle-shaped PAH with two embedded seven-membered rings.[15] For the azulene-embedded **1 d** not only a low-lying oxidation potential of +0.31 V was determined, but also two reduction processes at −1.36 V and −1.92 V vs. the ferrocene/ferrocenium couple were observed. Comparable potentials to the first oxidation and first reduction process of **1 d** were reported for non-planar azulene-embedded PAHs by Chi and coworkers[3c] and from the groups of Liu and Feng.[3d] The second reduction of **1 d** likely stems from the reduction of the corannulene moiety as for unsubstituted corannulene a single reduction process at a potential of −2.30 V is reported.[16]

We then investigated the optoelectronic properties of compounds **1 a**–**d** (Figure 3). Heptagon-embedded PAHs **1 a**–**c** absorb most strongly in the ultraviolet (UV) region with maxima between 290 and 300 nm and weak absorption bands between 400 and 420 nm being responsible for their yellow color. Enlargement of the π-system from benzene (**1 a**) to naphthalene (**1 c**) induces a very small bathochromic shift of 2–6 nm and leads to an increased extinction coefficient. An increase in electron density through dimethoxybenzene (**1 b**) has a larger influence and shifts maxima toward longer wavelengths, albeit at slightly decreased extinction coefficients. In stark contrast, azulene-containing **1 d** exhibits, in addition to strong absorption in the UV region, absorbance over the whole visible spectrum with maxima at 370 and 515 nm. Further, it possesses another maximum in the NIR region at 729 nm that extends to 950 nm. In the fluorescence measurements **1 a**–**c** exhibit blue (**1 a**, **1 c**) or green colors (**1 b**) and only slight differences in peak shape with maxima around 480–500 nm, Stokes shifts of around 4000 cm^{-1} and fluorescence quantum yields of 21–30 %. In contrast no fluorescence is observed for **1 d**, similar to pristine azulene which exhibits no fluorescence upon excitation to the S_1 state.[17]

Research Article
doi.org/10.1002/ejoc.202101273

In order to gain insight into the origin of the long-wavelength absorption of **1 d** we carried out theoretical investigations. Similar to **1 c**, *cisoid* and *transoid* configurations exist for **1 d** with the latter being disfavored by 19 kJ/mol. Therefore, for all calculations the *cisoid* form of **1 d** was used. TD-DFT calculations at the B3LYP/6-31 + G(d) level of theory attributed the NIR absorption of **1 d** to its HOMO–LUMO transition, similar to pristine azulene which gains its famous blue color from its weak S_1 transition.[18] Akin to azulene HOMO and LUMO of **1 d** are localized on different parts of the molecule. Strikingly though, the spatial distribution of frontier orbital coefficients is diametrical in both compounds: Whereas the HOMO of azulene is mainly located on its five-membered ring and the LUMO on the seven-membered ring, in **1 d** the HOMO resides mainly on the cyclohepta[*bc*]corannulene and the LUMO on the acenaphthylene moiety (see Supporting Information, Figure S23). Such uneven orbital coefficient distribution leads to charge transfer upon excitation which can be gauged by the Δr index.[19] For pristine azulene $\Delta r = 0.90$ Å was computed with electron density moving from the five- to the seven-membered ring, whereas for **1 d** a much longer charge transfer vector with $\Delta r = 2.39$ Å and opposite direction was obtained (Figure 4). This leads to the conclusion that for **1 d** the cyclohepta[*bc*]corannulene system serves as electron donor and the acenaphthylene moiety as electron acceptor during the excitation, contrary to pristine azulene.

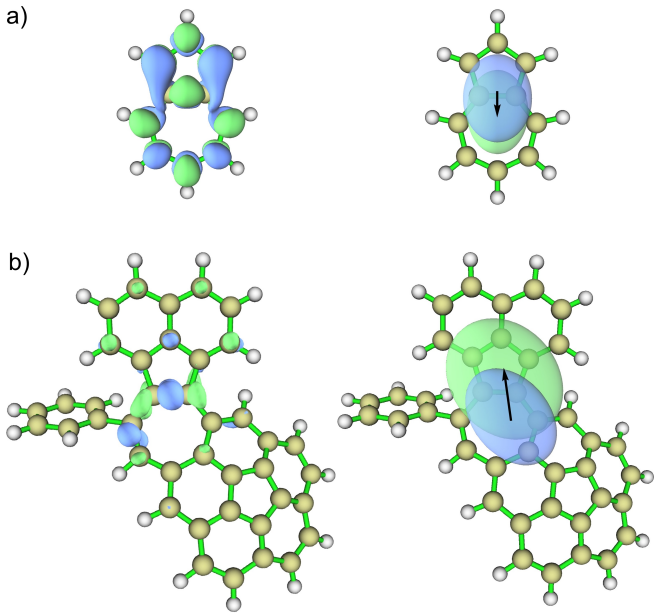

Figure 4. Charge density difference plots for the S_0–S_1 transition of azulene (a) with isovalue 0.08 and **1 d** (b) with isovalue 0.002/0.0005 calculated from TD-DFT data (B3LYP/6-31 + G(d)). Green and blue regions correspond to positive and negative changes in charge density, respectively. Individual nodes plotted on the left, barycenters on the right with vector arrows indicating the direction of charge transfer. Plots were created with multiwfn.[20]

The different UV/Vis/NIR spectra of **1 a–c** and **1 d** were further interpreted by calculations of nucleus-independent chemical shift (NICS)[21] and anisotropy of the induced current (AICD).[22] Due to the non-planarity of the molecules of interest the values for $NICS(1)_{zz}$ and $NICS(-1)_{zz}$ differ and were averaged out as $NICS(avg)_{zz}$ (see Supporting Information, Table S3).[23] While the odd-membered rings of **1 c** have strong antiaromatic character with high $NICS(avg)_{zz}$ values, those of the equivalent rings in **1 d** are slightly lower and thus less antiaromatic (Figure 5). Further, the five-membered ring in the azulene moiety of **1 d** has a higher nucleus-independent chemical shift than the corresponding ring in pristine acenaphthylene. These observations indicate that in **1 d** the aromaticity is stronger in the cyclohepta[*bc*]corannulene unit than that of **1 c** and the aromatic ring current is disconnected in the five-membered ring of acenaphthylene. Thus, when separated by the ring with the highest antiaromatic character, **1 d** can be seen as cyclohepta[*bc*]corannulene and naphthalene bridged by an antiaromatic five-membered ring, and **1 c** as corannulene and naphthalene bridged by an antiaromatic seven-membered ring.

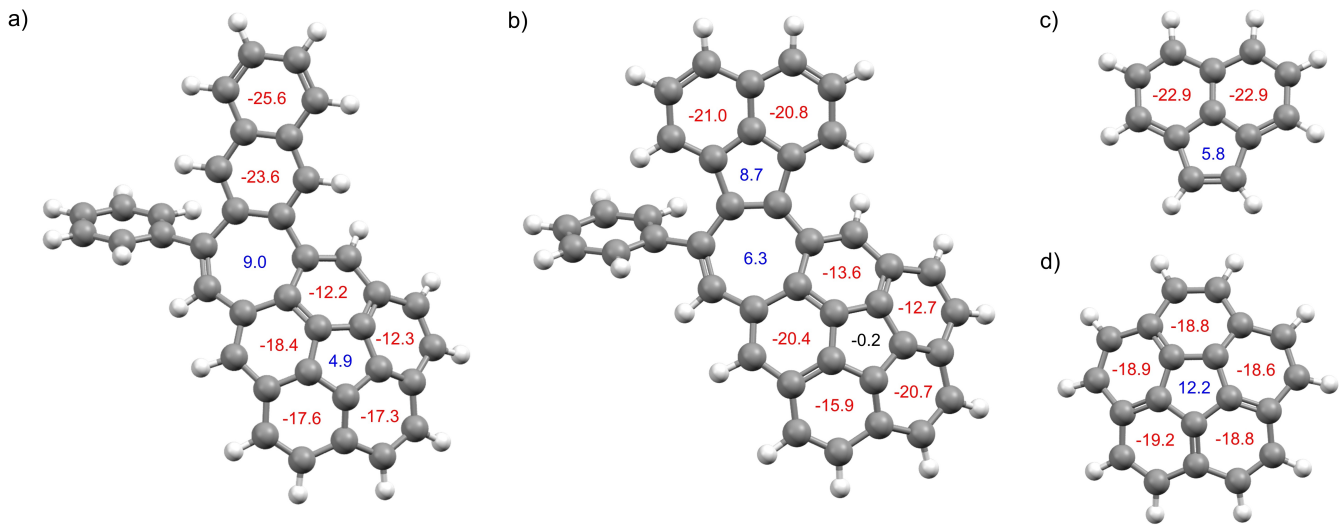

Figure 5. $NICS(avg)_{zz}$ values for **1 c** (a), **1 d** (b), acenaphthylene (c) and corannulene (d) calculated at the GIAO-B3LYP-6-31 + G(d) level of theory.

AICD plots corroborate this hypothesis (see Supporting Information, Figure S24).

Conclusion

In summary, we were able to establish a protocol for synthesizing PAHs bearing both positive and negative curvature. The positively curved corannulene-based borinic acid **5** could be extended by [5 + 2] annulation to form an additional seven-membered ring with negative curvature. We could analyse the geometry of **1c** using X-ray crystallographic analysis and confirmed the designed non-planar π-scaffold. Annulation with acenaphthylene resulted in azulene-embedded PAH **1d** with weak NIR absorption caused by its S_1 transition. Akin to its parent compound, the non-alternant character of **1d** leads to a lower energy transition with a charge transfer character. We anticipate that our method[8] may be useful to expand the scope of available non-planar PAHs with both positive and negative curvature and pave the way towards the investigation of such compounds.

Experimental Section

General procedure for the synthesis of 1a–d: To a Schlenk tube equipped with a magnetic stirring bar were added **5** (20.0 mg, 52.9 μmol, 1.0 equiv.), *ortho*-dibromoarene (106 μmol, 2.0 equiv.), $[Pd_2(dba)_3]\cdot CHCl_3$ (2.74 mg, 2.64 μmol, 5 mol%), $P(^tBu)_3\cdot HBF_4$ (1.69 mg, 5.82 μmol, 11 mol%) and cesium carbonate (56.9 mg, 174 μmol, 3.3 equiv.). Under nitrogen atmosphere distilled water (38.1 μL, 2.12 mmol, 40 equiv.) and *tert*-amyl alcohol (5 mL) were added by syringe. The mixture was stirred at room temperature for one hour and then at 100 °C for 42 h. After cooling to room temperature, it was filtered through Celite and the filter cake was washed with ethyl acetate. After evaporation of the solvent from the filtrate the crude solid was purified by flash chromatography on silica-gel (eluent cyclohexane/dichloromethane mixtures) and subsequent recycling GPC.

Acknowledgements

The authors are grateful for financial support from the Deutsche Forschungsgemeinschaft (Grant WU 317/23). Open Access funding enabled and organized by Projekt DEAL.

Conflict of Interest

The authors declare no conflict of interest.

Keywords: Annulation · Aromaticity · Azulene · Corannulene · Polycyclic aromatic hydrocarbons

[1] a) A. Narita, X.-Y. Wang, X. Feng, K. Müllen, *Chem. Soc. Rev.* **2015**, *44*, 6616–6643; b) G. Bottari, M. Á. Herranz, L. Wibmer, M. Volland, L. Rodríguez-Pérez, D. M. Guldi, A. Hirsch, N. Martín, F. D'Souza, T. Torres, *Chem. Soc. Rev.* **2017**, *46*, 4464–4500.
[2] K. Ziegler, K. Hafner, *Angew. Chem.* **1955**, *67*, 301–301.
[3] a) J. Liu, S. Mishra, C. A. Pignedoli, D. Passerone, J. I. Urgel, A. Fabrizio, T. G. Lohr, J. Ma, H. Komber, M. Baumgarten, C. Corminboeuf, R. Berger, P. Ruffieux, K. Müllen, R. Fasel, X. Feng, *J. Am. Chem. Soc.* **2019**, *141*, 12011–12020; b) X. Yang, F. Rominger, M. Mastalerz, *Angew. Chem. Int. Ed.* **2019**, *58*, 17577–17582; *Angew. Chem.* **2019**, *131*, 17741–17746; c) Y. Han, Z. Xue, G. Li, Y. Gu, Y. Ni, S. Dong, C. Chi, *Angew. Chem. Int. Ed.* **2020**, *59*, 9026–9031; *Angew. Chem.* **2020**, *132*, 9111–9116; d) J. Ma, Y. Fu, E. Dmitrieva, F. Liu, H. Komber, F. Hennersdorf, A. A. Popov, J. J. Weigand, J. Liu, X. Feng, *Angew. Chem. Int. Ed.* **2020**, *59*, 5637–5642; *Angew. Chem.* **2020**, *132*, 5686–5691; e) N. Ogawa, Y. Yamaoka, H. Takikawa, K.-i. Yamada, K. Takasu, *J. Am. Chem. Soc.* **2020**, *142*, 13322–13327; f) B. Pigulski, K. Shoyama, F. Würthner, *Angew. Chem. Int. Ed.* **2020**, *59*, 15908–15912; *Angew. Chem.* **2020**, *132*, 16042–16046; g) X. S. Zhang, Y. Y. Huang, J. Zhang, W. Meng, Q. Peng, R. Kong, Z. Xiao, J. Liu, M. Huang, Y. Yi, L. Chen, Q. Fan, G. Lin, Z. Liu, G. Zhang, L. Jiang, D. Zhang, *Angew. Chem. Int. Ed.* **2020**, *59*, 3529–3533; *Angew. Chem.* **2020**, *132*, 3557–3561; h) C. Zhu, K. Shoyama, F. Würthner, *Angew. Chem. Int. Ed.* **2020**, *59*, 21505–21509; *Angew. Chem.* **2020**, *132*, 21689–21693.
[4] a) M. Rickhaus, M. Mayor, M. Juricek, *Chem. Soc. Rev.* **2017**, *46*, 1643–1660; b) M. A. Majewski, M. Stepien, *Angew. Chem. Int. Ed.* **2019**, *58*, 86–116; *Angew. Chem.* **2019**, *131*, 90–122.
[5] a) K. Kawasumi, Q. Zhang, Y. Segawa, L. T. Scott, K. Itami, *Nat. Chem.* **2013**, *5*, 739–744; b) K. Kato, Y. Segawa, L. T. Scott, K. Itami, *Chem. Asian J.* **2015**, *10*, 1635–1639; c) J. M. Fernandez-Garcia, P. J. Evans, S. Medina Rivero, I. Fernandez, D. Garcia-Fresnadillo, J. Perles, J. Casado, N. Martin, *J. Am. Chem. Soc.* **2018**, *140*, 17188–17196; d) K. Kato, K. Takaba, S. Maki-Yonekura, N. Mitoma, Y. Nakanishi, T. Nishihara, T. Hatakeyama, T. Kawada, Y. Hijikata, J. Pirillo, L. T. Scott, K. Yonekura, Y. Segawa, K. Itami, *J. Am. Chem. Soc.* **2021**, *143*, 5465–5469.
[6] C. Chaolumen, I. A. Stepek, K. E. Yamada, H. Ito, K. Itami, *Angew. Chem. Int. Ed.* **2021**, *60*, 23508–23532, *Angew. Chem.* **2021**, *133*, 23700–23724.
[7] a) Y. T. Wu, J. S. Siegel, *Chem. Rev.* **2006**, *106*, 4843–4867; b) E. M. Muzammil, D. Halilovic, M. C. Stuparu, *Commun. Chem.* **2019**, *2*, 58.
[8] a) J. M. Farrell, D. Schmidt, V. Grande, F. Würthner, *Angew. Chem. Int. Ed.* **2017**, *56*, 11846–11850; *Angew. Chem.* **2017**, *129*, 12008–12012; b) J. M. Farrell, C. Mützel, D. Bialas, M. Rudolf, K. Menekse, A. M. Krause, M. Stolte, F. Würthner, *J. Am. Chem. Soc.* **2019**, *141*, 9096–9104.
[9] J. M. Farrell, V. Grande, D. Schmidt, F. Würthner, *Angew. Chem. Int. Ed.* **2019**, *58*, 16504–16507; *Angew. Chem.* **2019**, *131*, 16656–16659.
[10] V. Rajeshkumar, Y. T. Lee, M. C. Stuparu, *Eur. J. Org. Chem.* **2016**, *2016*, 36–40.
[11] D. Halilovic, M. Budanović, Z. R. Wong, R. D. Webster, J. Huh, M. C. Stuparu, *J. Org. Chem.* **2018**, *83*, 3529–3536.
[12] Deposition number 2115904 (for **1c**) contains the supplementary crystallographic data for this paper. These data are provided free of charge by the joint Cambridge Crystallographic Data Centre and Fachinformationszentrum Karlsruhe Access Structures service www.ccdc.cam.ac.uk/structures.
[13] R. G. Lawton, W. E. Barth, *J. Am. Chem. Soc.* **1971**, *93*, 1730–1745.
[14] F. H. Allen, O. Kennard, D. G. Watson, L. Brammer, A. G. Orpen, R. Taylor, *J. Chem. Soc. Perkin Trans. 2* **1987**, S1–S19.
[15] K. Y. Cheung, X. Xu, Q. Miao, *J. Am. Chem. Soc.* **2015**, *137*, 3910–3914.
[16] Y. Morita, S. Nishida, T. Kobayashi, K. Fukui, K. Sato, D. Shiomi, T. Takui, K. Nakasuji, *Org. Lett.* **2004**, *6*, 1397–1400.
[17] G. Viswanath, M. Kasha, *J. Chem. Phys.* **1956**, *24*, 574–577.
[18] J. Michl, E. W. Thulstrup, *Tetrahedron* **1976**, *32*, 205–209.
[19] C. A. Guido, P. Cortona, B. Mennucci, C. Adamo, *J. Chem. Theory Comput.* **2013**, *9*, 3118–3126.
[20] T. Lu, F. Chen, *J. Comput. Chem.* **2012**, *33*, 580–592.
[21] Z. Chen, C. S. Wannere, C. Corminboeuf, R. Puchta, P. v. R. Schleyer, *Chem. Rev.* **2005**, *105*, 3842–3888.
[22] D. Geuenich, K. Hess, F. Köhler, R. Herges, *Chem. Rev.* **2005**, *105*, 3758–3772.
[23] M. Antić, B. Furtula, S. Radenković, *J. Phys. Chem. A* **2017**, *121*, 3616–3626.

Manuscript received: October 15, 2021
Revised manuscript received: December 7, 2021